

Article

Study on the Influence of an Under-Crossing Parallel Double-Line Shield Tunnel on the Existing Tunnel Structure

Linhai Zeng ^{1,2,*}, Daobing Zhang ¹ , Changjiang Lian ², Jiahua Zhang ³ and Huadong Yin ¹

¹ School of Resource Environment and Safety Engineering, Hunan University of Science and Technology, Xiangtan 411201, China; dbzhang@hnust.edu.cn (D.Z.); 21020101030@mail.hnust.edu.cn (H.Y.)

² Guangdong Zhonggong Architectural Design Institute Co., Ltd., Guangzhou 510700, China

³ Work Safety Key Lab on Prevention and Control of Gas and Roof Disasters for Southern Coal Mines, Hunan Provincial Key Laboratory of Safe Mining Techniques of Coal Mines, Hunan University of Science and Technology, Xiangtan 411201, China; 1010090@hnust.edu.cn

* Correspondence: 22300101005@mail.hnust.edu.cn; Tel.: +86-13902203157

Abstract: Extra care should be taken when new tunnels pass through an existing tunnel. If it is not handled properly, this will affect the operation safety of the existing line, and bring security risks to the train's operation. In order to study the impact of an under-crossing parallel double-line shield tunnel on the existing shield tunnel structure, the influence of tunnel construction on the deformation of overlying strata was analyzed, and the formula for estimating the formation settlement at depth Z below the surface, caused by the excavation of a double-tunnel parallel tunnel, was deduced. Then, a series of three-dimensional finite element numerical simulations were carried out. We analyzed and systematically studied the adverse effects of the tunnel structure of Guangzhou subway Line 5, caused by the tunneling of subway Line 18, evaluated its structure and operational safety, and provided suggestions for site construction. This research demonstrates the following conclusions. (1) The tunnel structures of subway Line 5 and Line 18 are mainly in the strongly weathered argillaceous siltstone stratum, and lightly weathered argillaceous siltstone stratum, respectively, and the stratum where the Line 18 tunnel is located is relatively safe. (2) According to three-dimensional finite element numerical simulation analysis, during the shield-tunneling process of subway Line 18, the maximum X horizontal displacement, the maximum Y horizontal displacement, and the maximum Z vertical displacement of the tunnel structure in subway Line 5 are 1.09, 3.50, and 4.55 mm, respectively. It is considered that the impact of the shield-tunnel penetration of subway Line 18 on the tunnel structure of subway Line 5 is relatively controllable, and does not affect the structure and operational safety. (3) It is suggested that settlement monitoring should be strengthened within the range of 12 m (about 1.5 tunnel diameter D). before and after the excavation axis of the underpass tunnel, and it is necessary to carry out local reinforcement treatment, to prevent adverse effects on the operation of the existing tunnel.

Keywords: shield tunnel; under-crossing; three-dimensional numerical modelling; displacement monitoring; ground settlements

MSC: 00A71



Citation: Zeng, L.; Zhang, D.; Lian, C.; Zhang, J.; Yin, H. Study on the Influence of an Under-Crossing Parallel Double-Line Shield Tunnel on the Existing Tunnel Structure. *Mathematics* **2023**, *11*, 3125. <https://doi.org/10.3390/math11143125>

Academic Editors: Yuexiang Lin, Jianjun Ma, Mingfeng Lei and Chengyong Cao

Received: 15 June 2023
Revised: 10 July 2023
Accepted: 12 July 2023
Published: 14 July 2023



Copyright: © 2023 by the authors. Licensee MDPI, Basel, Switzerland. This article is an open access article distributed under the terms and conditions of the Creative Commons Attribution (CC BY) license (<https://creativecommons.org/licenses/by/4.0/>).

1. Introduction

Urban rail transit is recognized around the world as a form of “green transportation”, with low energy consumption and less pollution. Urban rail transit construction in China has entered a period of rapid and concentrated development. A shield tunnel is safe, efficient, and can be applied to a variety of strata, and has been widely used in urban rail transit construction [1–6]. Nowadays, more and more new rail transit lines pass through existing buildings, and managing the construction of this section of the underpass structure is often the key to determining the duration of the entire line. When the new subway tunnel

passes through the existing subway structure, extra care should be taken. If this is not handled properly, the service safety of the existing line will be affected and, in serious cases, it will bring potential safety hazards to the train operation [7–9].

In recent years, research on the influence of new rail transit systems on existing buildings, and on the upper rock and soil mass, has become an important topic in the field of rail transit safety. Liu et al. [10] used three-dimensional finite element analysis to study the interactions between vertical cross tunnels. The study showed that in areas with high horizontal stress, a new tunnel would cause the shotcrete lining of the existing tunnel to be stretched on the side toward the tunnel opening, and compressed at the vault and invert. Zhang and Huang [3] studied the soil disturbance caused by multi-line tunnel construction in a soft-soil area, and the interaction mechanism for adjacent structures, such as the existing above-crossing and down-crossing subway tunnels. Similarly, there are many cases in which new rail transit under-crosses existing tunnels, which have been studied by many scholars [11–22]. For example, Lai et al. [23] proposed a new method for predicting the ground settlement caused by double tunnels penetrating the existing tunnel, on the basis of a comprehensive consideration of the coupling effect of the front tunnel, the intermediate soil mass, the back tunnel, and the existing tunnel. Ng et al. [11] used the finite element numerical simulation method to study the influence of the size of the existing horseshoe tunnel on the interaction of the circular cross tunnel. Yin et al. [24] studied the influence of the tunneling clearance of an under-construction shield tunnel on the existing shield tunnel, and found that the plastic development of the soil through the existing tunnel structure had a significant influence on the settlement of the overlying soil. Lin et al. [25] studied the influence of the cross angle of the new and old tunnels on the deformation characteristics of existing tunnels. Gan et al. [26] studied the deformation by the new tunnel of the existing longitudinal tunnel, by considering the asymmetric surface settlement.

However, there are few studies on the impact of rail transit shield tunneling on the existing rail transit tunnel structure, and safety analysis. The Guangzhou subway Line 18 Pazhou West Station–Xiancun Station, under the existing subway Line 5 Zhujiang New City station–Lide station tunnel, may have a negative impact on the subway Line 5 tunnel structure. Therefore, this paper carries out a series of three-dimensional finite element numerical simulation analyses, based on the shield-tunneling characteristics of subway Line 18, and systematically studies the adverse impact of the shield-tunneling structure of Subway Line 18 under-crossing subway Line 5, evaluates its structure and operation safety, and provides safety measures, and suggestions for the on-site construction.

2. Engineering Background

Guangzhou Subway Line 18 starts at Wanqingsha Junction in Nansha, and ends at Tianhe Guangzhou East Station. The total length of the line is 61.3 km, all of which consist of underground lines, with nine stations. The Pazhou West District Station–Xian Cun Station section of Guangzhou Subway Line 18 under-crosses the Zhujiang New Town Station–Lide Station section tunnel of the existing Subway Line 5. In this section, the diameter of the shield is 8.5 m, the average buried depth of the tunnel roof is about 25 m, and the tunnel body is mainly lightly weathered argillaceous siltstone and gravel. The distance from the tunnel floor of subway Line 5 above is only about 3.5 m, on average.

According to the geological survey and relevant data on site, the following charts were drawn, to clarify the positional relationship between Subway Line 18 and Subway Line 5. Figures 1 and 2 show the two-dimensional and three-dimensional position diagrams of the two subway lines, respectively.

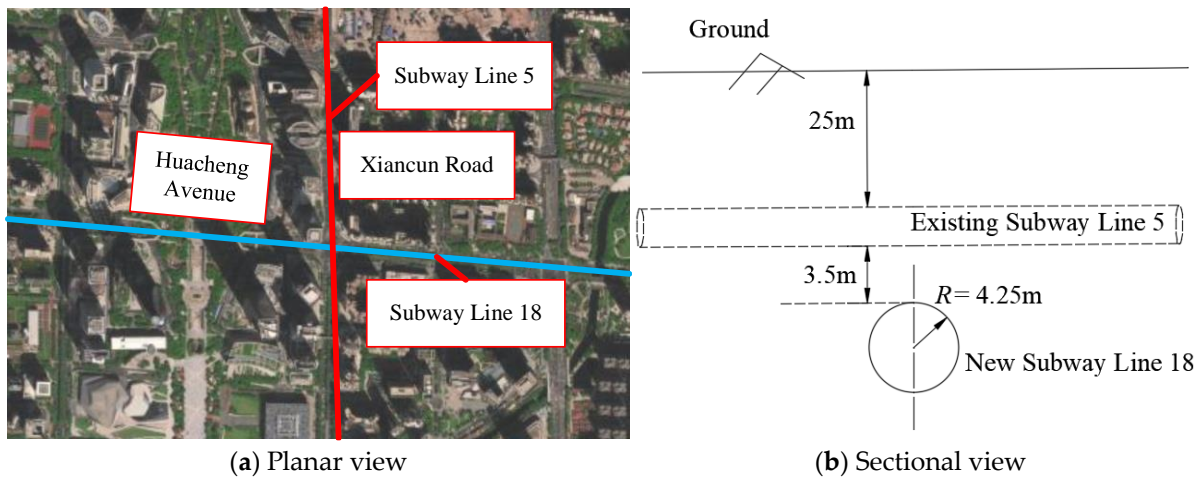


Figure 1. A two-dimensional position relation diagram of Subway Line 18 and Subway Line 5.

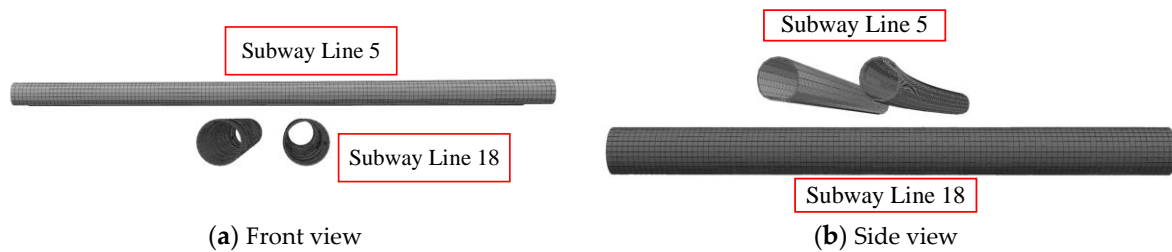


Figure 2. Three-dimensional position relation diagram of Subway Line 18 and Subway Line 5.

The area surrounding the site mainly comprises municipal roads and bridges, office buildings, residences, and shops, and the terrain is relatively flat. The main soil layers through the site are as follows: ① miscellaneous fill <1-1>, ② silty clay <2-4>, ③ strongly weathered argillaceous siltstone <7-3>, and ④ slightly weathered argillaceous siltstone <9-3>. The profile of the main soil layer of the site can be seen in Figure 3. The structure of subway Line 5 is mainly located in the strongly weathered argillaceous siltstone layer, which is extremely soft rock, and the basic quality grade of the rock mass is V. The structure of subway Line 18 is mainly located in the slightly weathered argillaceous siltstone layer. The rock hardness is classified as being between soft rock and relatively hard rock, and the basic quality grade of the rock mass is IV.

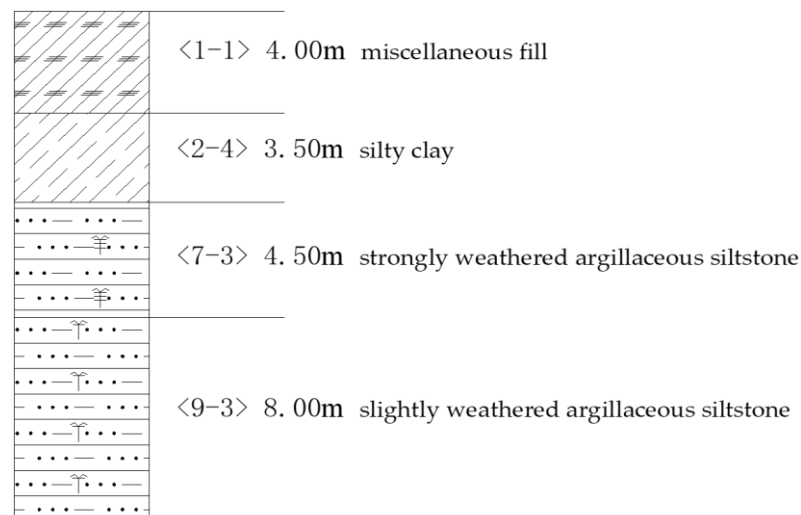


Figure 3. The profile of the main soil layers at the site.

3. Analysis of Influence of Tunnel Construction on Overlying Strata Deformation

When the shield tunneling under-crosses the existing tunnel, its construction influence range includes the direction of the shield-tunneling machine (longitudinal length S), and the direction of the axis perpendicular to the tunnel-tunneling machine (transverse width W). Peck [27] analyzed and summarized a large number of measured data in 1969, and believed that the transverse settlement trough curve of the surface basically accords with Gaussian distribution. Later, in 1982, Attewell [28] presented a summary and analysis of shield construction cases; the results show that the surface longitudinal settlement deformation curve basically accords with Gaussian distribution, with the theoretical value S of the disturbance length in front of the excavation face, as shown in Figure 4:

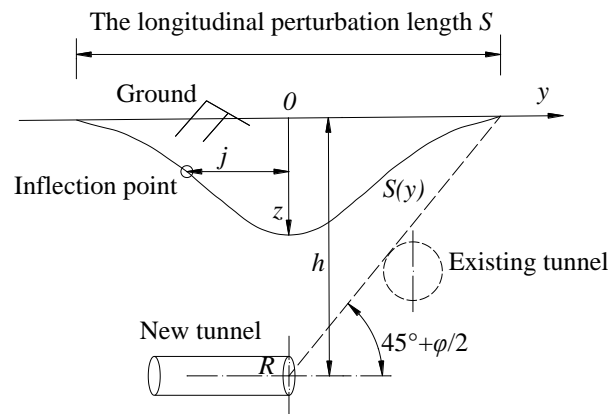


Figure 4. The schematic diagram of the longitudinal disturbance length when the shield underpasses the existing tunnel.

In this case, the soil displacement direction is toward the shield working face, the geological action is manifested as ground settlement, and the disturbance length is the theoretical lower limit. The other case is that the soil displacement direction is far away from the shield working face, the geological action shows the ground uplift, and the disturbance length is the theoretical upper limit.

The theoretical value of the transverse disturbance width W can be divided into two types of disturbance width: when the soil moves to both sides of the shield extrusion (the theoretical upper limit value), and when the soil moves to the center of the tunnel after the shield passes through (the theoretical lower limit value). Figure 5 shows the schematic diagram of the transverse disturbance width perpendicular to the tunnel axis, when the shield underpasses the existing tunnel.

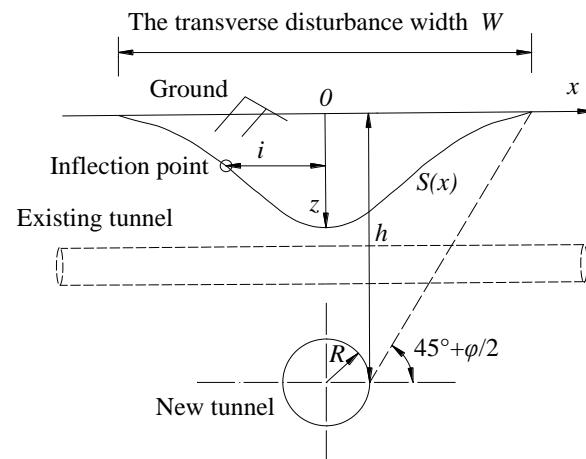


Figure 5. The schematic diagram of the transverse disturbance width perpendicular to the tunnel axis, when the shield tunneling underpasses the existing tunnel.

The influence range of ground disturbance in shield construction can be solved according to the following equation:

$$\begin{aligned}
 S &= htg(45^\circ + \varphi/2) \text{ theoretical upper limit value} \\
 S &= htg(45^\circ - \varphi/2) \text{ theoretical lower limit value} \\
 W &= R + htg(45^\circ + \varphi/2) \text{ theoretical upper limit value} \\
 W &= R + htg(45^\circ - \varphi/2) \text{ theoretical lower limit value}
 \end{aligned}
 \tag{1}$$

where S and W are the disturbance length in front of the excavation face, and the disturbance width perpendicular to the tunnel axis, respectively; h is the buried depth of the tunnel axis; φ is the internal friction angle of the soil; and R is the tunnel radius.

In fact, during shield excavation, the supporting force of the face at this position is generally greater than the earth pressure, and the soil in front of the face is under passive compression, so the theoretical value of the disturbance length in front of the face should be:

$$\begin{aligned}
 S &= (h + R)tg(45^\circ + \varphi/2) \text{ theoretical upper limit value} \\
 S &= (h + R)tg(45^\circ - \varphi/2) \text{ theoretical lower limit value}
 \end{aligned}
 \tag{2}$$

In actual shield tunneling, the disturbance range of the soil is between the theoretical upper limit and the lower limit.

3.1. Empirical Formula for Surface Transverse Settlement

The formula for estimating the distribution of the surface transverse settlement, proposed by Peck [27], is as follows:

$$S(x) = S_{\max}e^{(-\frac{x^2}{2i^2})},
 \tag{3}$$

where $S(x)$ is the surface settlement value at the place x from the tunnel excavation point to the origin; S_{\max} is the maximum ground settlement during the tunnel excavation; x is the horizontal distance from the tunnel excavation point to the tunnel center; and i is the width coefficient of the settlement trough; that is, the distance between the bending point and the origin in the surface settlement distribution curve.

The schematic diagram of the transverse distribution of the ground settlement after tunnel excavation is shown in Figure 6.

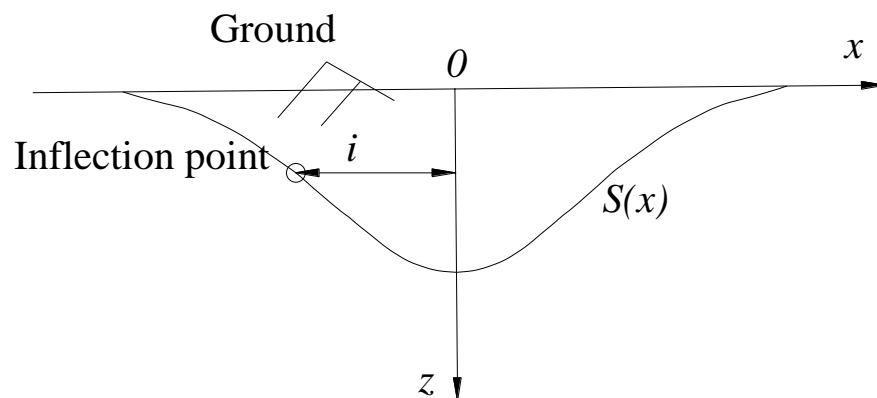


Figure 6. The schematic diagram of the surface settlement and transverse distribution of the stratum deformation after tunnel excavation.

This estimation formula assumes that the surface settlement tank per unit length caused by tunnel excavation, when not drained, is equal to the corresponding formation loss volume V_l , thus:

$$\begin{aligned}
 V_l &= \int_{-\infty}^{+\infty} S_{\max} \exp\left(-\frac{x^2}{2i^2}\right) dx = i\sqrt{2\pi}S_{\max} \\
 V_l &= \pi R^2 \eta \\
 i &= \frac{h}{\sqrt{2\pi}tg(45^\circ - \varphi/2)}
 \end{aligned}
 \tag{4}$$

where V_l is the formation loss volume caused by tunnel excavation per unit length; and η is the formation loss rate.

However, it is difficult to predict the settlement of deep soil using Peck’s estimation formula so, according to Peck’s formula, the estimation formula of the formation settlement at depth z below the surface can be written as follows:

$$\begin{aligned}
 S_z(x) &= S_{\max}(z) \exp\left\{-\frac{x^2}{2i(z)^2}\right\} \\
 S_{\max}(z) &= \frac{V_l}{\sqrt{2\pi}i(z)}
 \end{aligned}
 \tag{5}$$

where $S_z(x)$ is the surface settlement value of the tunnel excavation center at depth z below the surface; $S_{\max}(z)$ is the maximum surface settlement value at the center of the tunnel excavation face at a depth of z below the surface; and $i(z)$ is the width coefficient of the settling trough at depth z below the surface.

Based on the superposition principle, New and O’Reilly [29] proposed the following formula for calculating the lateral settlement of the surface caused by the excavation of double-hole parallel tunnels, when the shield underpasses the existing tunnel engineering without considering the interaction effect:

$$S(x) = \frac{A_1 V_{l1}}{\sqrt{2\pi}i_1} \exp\left[-\frac{(x - D/2)^2}{2i_1^2}\right] + \frac{A_2 V_{l2}}{\sqrt{2\pi}i_2} \exp\left[-\frac{(x + D/2)^2}{2i_2^2}\right],
 \tag{6}$$

where A_1 and A_2 are the cross section areas of tunnel 1 and tunnel 2, respectively; V_{l1} and V_{l2} are the formation loss rates caused by the construction of tunnel 1 and tunnel 2, respectively; i_1 and i_2 are the width coefficients of the settling trough caused by tunnel 1 and tunnel 2 excavations, respectively; and D is the distance between the centers of the two tunnels.

The schematic diagram of the surface settlement and transverse stratum deformation after the excavation of a double-cave parallel tunnel is shown in Figure 7:

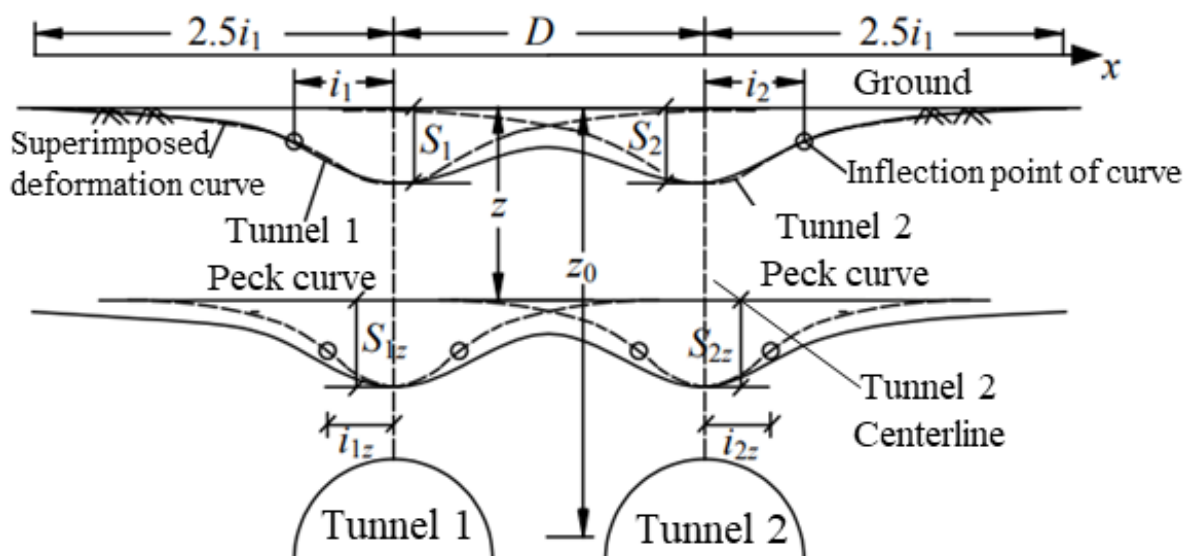


Figure 7. The surface settlement by the superposition of two side-by-side tunnels.

According to Equations (5) and (6), the formula for estimating the formation settlement at depth z below the surface, caused by double-line parallel tunnel excavation, is as follows:

$$S_z(x) = \frac{A_1 V_{l1}}{\sqrt{2\pi}i_1(z)} \exp\left[-\frac{(x - D/2)^2}{2i_1^2(z)}\right] + \frac{A_2 V_{l2}}{\sqrt{2\pi}i_2(z)} \exp\left[-\frac{(x + D/2)^2}{2i_2^2(z)}\right], \quad (7)$$

where $i_1(z)$ and $i_2(z)$ are the width coefficients of the settlement trough at depth z below the surface of tunnel 1 and tunnel 2, respectively.

3.2. Empirical Formula of Surface Longitudinal Settlement

The estimation formula of the surface longitudinal settlement, proposed by Attewell [28], is written as follows:

$$S(y) = S_{\max} \left[\Phi\left(\frac{y - y_i}{j}\right) - \Phi\left(\frac{y - y_f}{j}\right) \right], \quad (8)$$

where $S(y)$ is the longitudinal settlement of the surface at the coordinate position y in front of the palm face; y denotes the ground surface coordinates along the tunnel construction direction; y_i is the starting point of shield tunnel construction; y_f is the length of the distance between the palm surface and the origin of the coordinate axis during shield construction; j is the width coefficient of the longitudinal settlement trough caused by shield excavation; and Φ is the standard normal distribution function.

Liu and Hou [30] revised Attewell’s estimation formula of longitudinal surface settlement, based on relevant practical engineering cases in Shanghai:

$$S(y) = \frac{V_{la}}{\sqrt{2\pi}j} \left[\Phi\left(\frac{y - y_j}{j}\right) - \Phi\left(\frac{y - y_f}{j}\right) \right] + \frac{V_{lb}}{\sqrt{2\pi}j} \left[\Phi\left(\frac{y - y'_j}{j}\right) - \Phi\left(\frac{y - y'_f}{j}\right) \right], \quad (9)$$

where L_S is the length of the shield, $y'_j = y_j - L_S$, $y'_f = y_f - L_S$; V_{la} is the stratum loss caused by the face of the palm; and V_{lb} is the soil loss caused by insufficient void grouting at the tail of the shield machine, and the change in construction direction of the shield machine.

Similarly, according to the derivation of the estimation formula for lateral settlement, the estimation formula for the vertical settlement of the stratum at the depth of z below the surface can be written as:

$$S(y) = \frac{V_{la}}{\sqrt{2\pi}j(z)} \left[\Phi\left(\frac{y - y_j}{j(z)}\right) - \Phi\left(\frac{y - y_f}{j(z)}\right) \right] + \frac{V_{lb}}{\sqrt{2\pi}j(z)} \left[\Phi\left(\frac{y - y'_j}{j(z)}\right) - \Phi\left(\frac{y - y'_f}{j(z)}\right) \right], \quad (10)$$

where $j(z)$ is the width coefficient of the longitudinal settlement trough of the stratum at depth z below the surface.

According to the superposition principle, the calculation formula of the surface longitudinal settlement caused by double-line parallel tunnel excavation is as follows:

$$S(y) = \frac{A_1 V_{la}}{\sqrt{2\pi}j_1} \left[\Phi\left(\frac{y - y_j - D/2}{j_1}\right) - \Phi\left(\frac{y - y_f - D/2}{j_1}\right) \right] + \frac{A_1 V_{lb}}{\sqrt{2\pi}j_1} \left[\Phi\left(\frac{y - y'_j - D/2}{j_1}\right) - \Phi\left(\frac{y - y'_f - D/2}{j_1}\right) \right] + \frac{A_2 V_{la}}{\sqrt{2\pi}j_2} \left[\Phi\left(\frac{y - y_j + D/2}{j_2}\right) - \Phi\left(\frac{y - y_f + D/2}{j_2}\right) \right] + \frac{A_2 V_{lb}}{\sqrt{2\pi}j_2} \left[\Phi\left(\frac{y - y'_j + D/2}{j_2}\right) - \Phi\left(\frac{y - y'_f + D/2}{j_2}\right) \right], \quad (11)$$

where j_1 and j_2 are the width coefficients of the longitudinal settlement trough caused by the construction of tunnel 1 and tunnel 2, respectively.

According to Equations (10) and (11), the formula for estimating the formation longitudinal settlement at depth z below the surface caused by double-line parallel tunnel excavation is as follows:

$$S_{(z)}(y) = \frac{A_1 V_{1a}}{\sqrt{2\pi}j_1(z)} \left[\Phi\left(\frac{y-y_j-D/2}{j_1(z)}\right) - \Phi\left(\frac{y-y_f-D/2}{j_1(z)}\right) \right] + \frac{A_1 V_{1b}}{\sqrt{2\pi}j_1(z)} \left[\Phi\left(\frac{y-y'_j-D/2}{j_1(z)}\right) - \Phi\left(\frac{y-y'_f-D/2}{j_1(z)}\right) \right] + \frac{A_2 V_{2a}}{\sqrt{2\pi}j_2(z)} \left[\Phi\left(\frac{y-y'_j+D/2}{j_2(z)}\right) - \Phi\left(\frac{y-y'_f+D/2}{j_2(z)}\right) \right] + \frac{A_2 V_{2b}}{\sqrt{2\pi}j_2(z)} \left[\Phi\left(\frac{y-y'_j+D/2}{j_2(z)}\right) - \Phi\left(\frac{y-y'_f+D/2}{j_2(z)}\right) \right] \quad (12)$$

where $j_1(z)$ and $j_2(z)$ are the width coefficients of the longitudinal settlement trough of the stratum at depth z below the surface caused by the construction of tunnel 1 and tunnel 2, respectively.

4. Three-Dimensional Numerical Analysis of the Influence of an Under-Crossing Parallel Double-Line Shield Tunnel on the Existing Tunnel Structure

4.1. Three-Dimensional Numerical Model

According to the tunnel structure of subway Line 5, and the shield-tunneling construction characteristics of subway Line 18, MIDAS 4.0 numerical simulation software is used to establish a three-dimensional finite element calculation model. The model is described as follows:

(1) The strata in the calculation model mainly include ① miscellaneous fill <1-1>, ② silty clay <2-4>, ③ strongly weathered argillaceous siltstone <7-3> and ④ slightly weathered argillaceous siltstone <9-3>. The parameters calculated for each rock and soil layer are shown in Table 1. The tunnel cross-section of subway Line 18 and subway Line 5 in this model is circular, and the radius R is 4.25 m and 2.75 m, respectively.

Table 1. The basic physical and mechanical parameters of rock and soil layers.

Layer No.	Rock and Soil Layer Name	Layer Thickness (m)	Volume Weight γ (kN/m ³)	Young's Modulus E (MPa)	Poisson's Ratio μ	Cohesion c (kPa)	Internal Friction Angle φ (°)
①	miscellaneous fill	4.00	19.5	10.0	0.38	10.0	15.0
②	silty clay	3.50	18.5	15.0	0.36	15.0	17.0
③	strongly weathered argillaceous siltstone	4.50	21.0	70.0	0.28	30.0	22.0
④	slightly weathered argillaceous siltstone	8.00	25.0	5000.0	0.19	500.0	30.0

(2) The boundary conditions of the calculation model are as follows: X-direction constraints on the left and right sides of the model, Y-direction constraints on the front and back of the model, and Z-direction displacement constraints at the bottom of the model. The calculation range is as follows: the X-direction boundary length is 200 m, the Y-direction boundary length is 200 m, and the Z-direction boundary length is 80 m.

(3) The model satisfies the following assumptions: (a) the surrounding rock is an ideal elastic-plastic material, and the Mohr-Coulomb model is used for modeling; (b) the model material adopts the isotropic hypothesis; (c) no earthquake occurs during the shield construction of the Subway Line 18 tunnel; (d) in the initial ground stress analysis, only the gravity stress of the existing buildings and rock mass is calculated, and the effect of groundwater is ignored; and € no time effect is taken into account.

(4) Based on the initial ground stress field of the site, the maximum X horizontal displacement, maximum Y horizontal displacement, maximum Z vertical displacement, and maximum total displacement of the tunnel structure of subway Line 5, in the process of the shield tunneling of subway Line 18, were obtained, to evaluate the safety impact of the shield tunneling of subway Line 18 on the tunnel structure of subway Line 5.

(5) The study conditions include: analysis of the initial ground stress field of the site (after the calculation was completed, the soil and structural displacement were reset to zero), the completion of construction on subway Line 5 (after the calculation was completed, the soil and structural displacement was reset to zero), and the subway Line 18 tunnel excavation at 12 m, 24 m, 36 m, 42 m, 48 m, 54 m, 60 m, 66 m, 78 m, 90 m, and 102 m, respectively.

Figure 8 is the effect drawing of the three-dimensional finite element model.

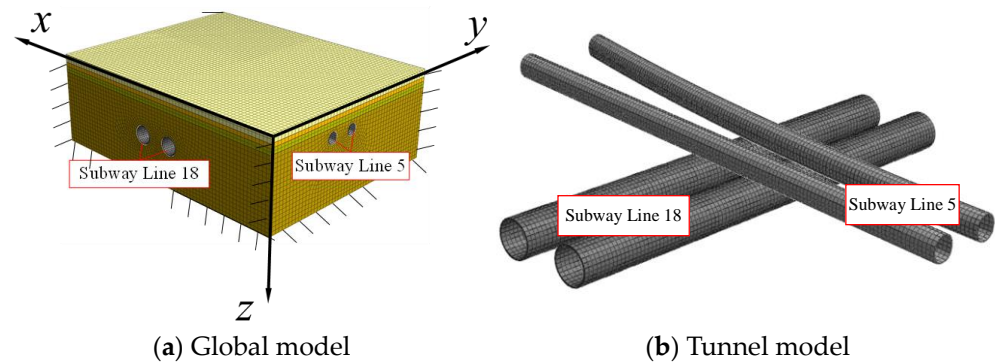


Figure 8. The effect drawing of the three-dimensional finite element model.

4.2. Analysis and Conclusion of Three-Dimensional Numerical Results

4.2.1. Displacement Analysis of Existing Subway Tunnels

According to the research conditions, the cloud map of the maximum X horizontal displacement, maximum Y horizontal displacement, maximum Z vertical displacement, and maximum total displacement of the tunnel structure of subway Line 5 in the shield tunneling process of subway Line 18 can be obtained through three-dimensional finite element numerical simulation. Due to the limited space in this paper, only the maximum Y horizontal displacement and maximum Z vertical displacement of the tunnel structure of subway Line 5 in the shield-tunneling process of subway Line 18 are listed (Figures 9 and 10).

As can be seen from Figure 1, the minimum clear distance between the new tunnel and the existing tunnel is only 3.5 m, which is 0.41 times the diameter D of the new tunnel, and less than $0.5D$. Close-range construction will result in a slight uplift of the lining of the existing tunnel-surrounding rock above. With the increase in excavation mileage, the amount of uplift will rise slowly, but the total amount of uplift will be small. The maximum uplift is located near the vault and arch waist (see subway Line 18 shield excavation to 24 m in Figure 10), which is approximately 0.1 mm. The excavation of a new tunnel that undergoes the existing tunnel will cause obvious settlement in the existing tunnel, and the maximum settlement is around the arch bottom and waist, which is approximately 4.55 mm (see subway Line 18 shield excavation to 102 m, in Figure 10). The left and right lines of the new tunnel are excavated at the same time. The left and right lines of the tunnel are almost parallel, and the crossing angle with the existing tunnel above is approximately a right angle (orthogonal). Therefore, surrounding-rock deformation will occur in the overlapping area during excavation, and special technical measures must be taken to control it, otherwise it will have adverse effects on the existing tunnel above.

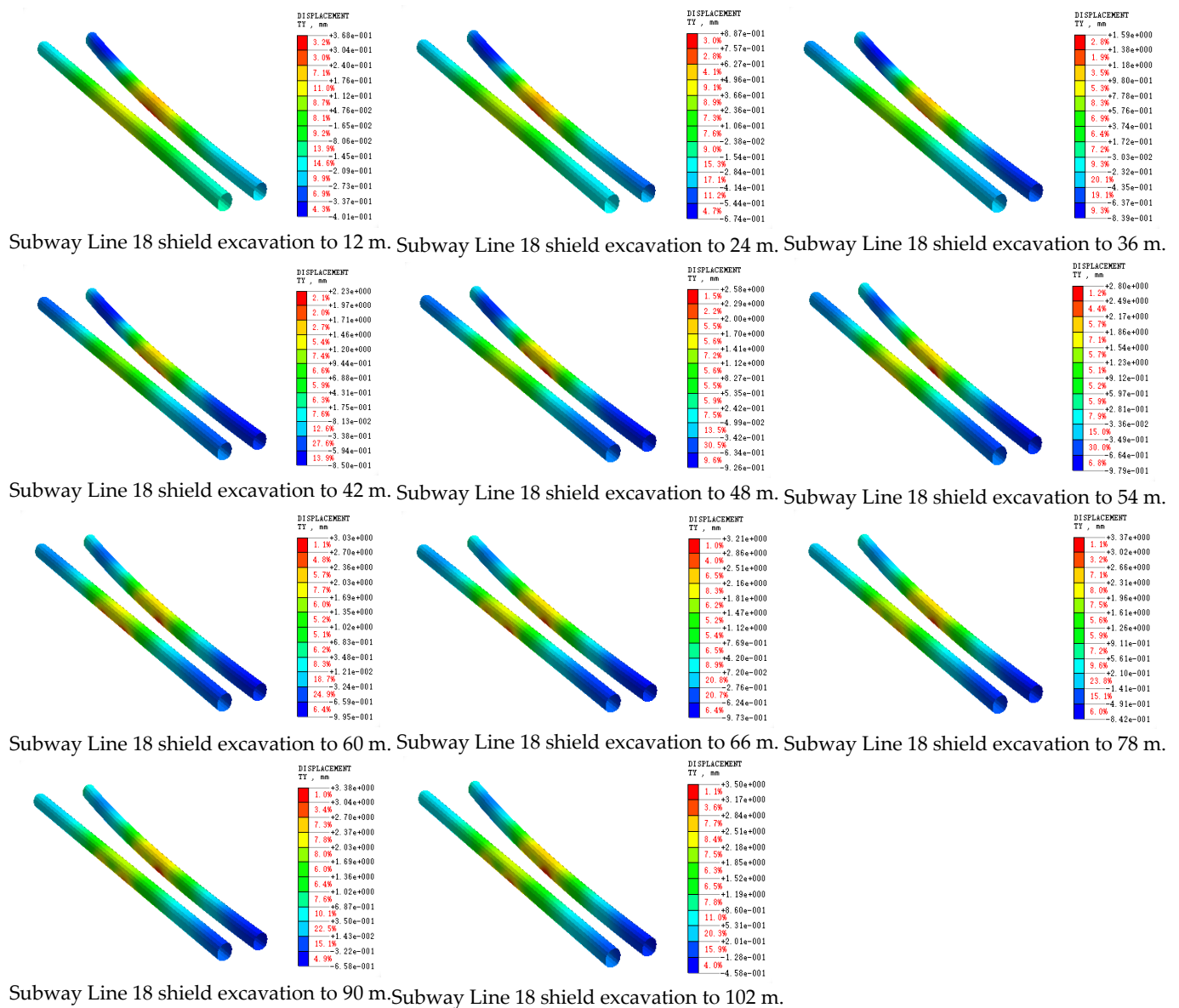


Figure 9. The maximum Y horizontal displacement nephogram of the tunnel structure of subway Line 5 during the tunneling process of subway Line 18.

According to the simulation results, the displacement parameters of the tunnel structure in subway Line 5 during the shield tunneling of subway Line 18 were obtained, and the data were plotted in the following table (Table 2).

Table 2. Summary of the maximum displacement of the tunnel structure of subway Line 5 during the shield tunneling of subway Line 18.

Simulated Working Condition	Maximum Displacement (mm)			
	Horizontal X Displacement	Horizontal Y Displacement	Vertical Z Displacement	Total Displacement
Analysis of initial ground stress field of site	0.000	0.000	0.000	0.000
Construction of subway Line 5 has been completed	0.000	0.000	0.000	0.000
Subway Line 18 tunnel excavation 12 m	−0.105	−0.401	−0.191	−0.421
Subway Line 18 tunnel excavation 24 m	−0.256	−0.887	−0.561	−0.956
Subway Line 18 tunnel excavation 36 m	−0.533	−1.59	−1.43	−1.83

Table 2. Cont.

Simulated Working Condition	Maximum Displacement (mm)			
	Horizontal X Displacement	Horizontal Y Displacement	Vertical Z Displacement	Total Displacement
Subway Line 18 tunnel excavation 42 m	-0.701	-2.23	-1.93	-2.40
Subway Line 18 tunnel excavation 48 m	-0.833	-2.58	-2.44	-2.81
Subway Line 18 tunnel excavation 54 m	-0.931	-2.80	-2.95	-3.33
Subway Line 18 tunnel excavation 60 m	-1.00	-3.03	-3.43	-4.02
Subway Line 18 tunnel excavation 66 m	-1.05	-3.21	-3.79	-4.61
Subway Line 18 tunnel excavation 78 m	-1.09	-3.37	-4.33	-5.20
Subway Line 18 tunnel excavation 90 m	-1.09	-3.38	-4.49	-5.32
Subway Line 18 tunnel excavation 102 m	-1.09	-3.50	-4.55	-5.43

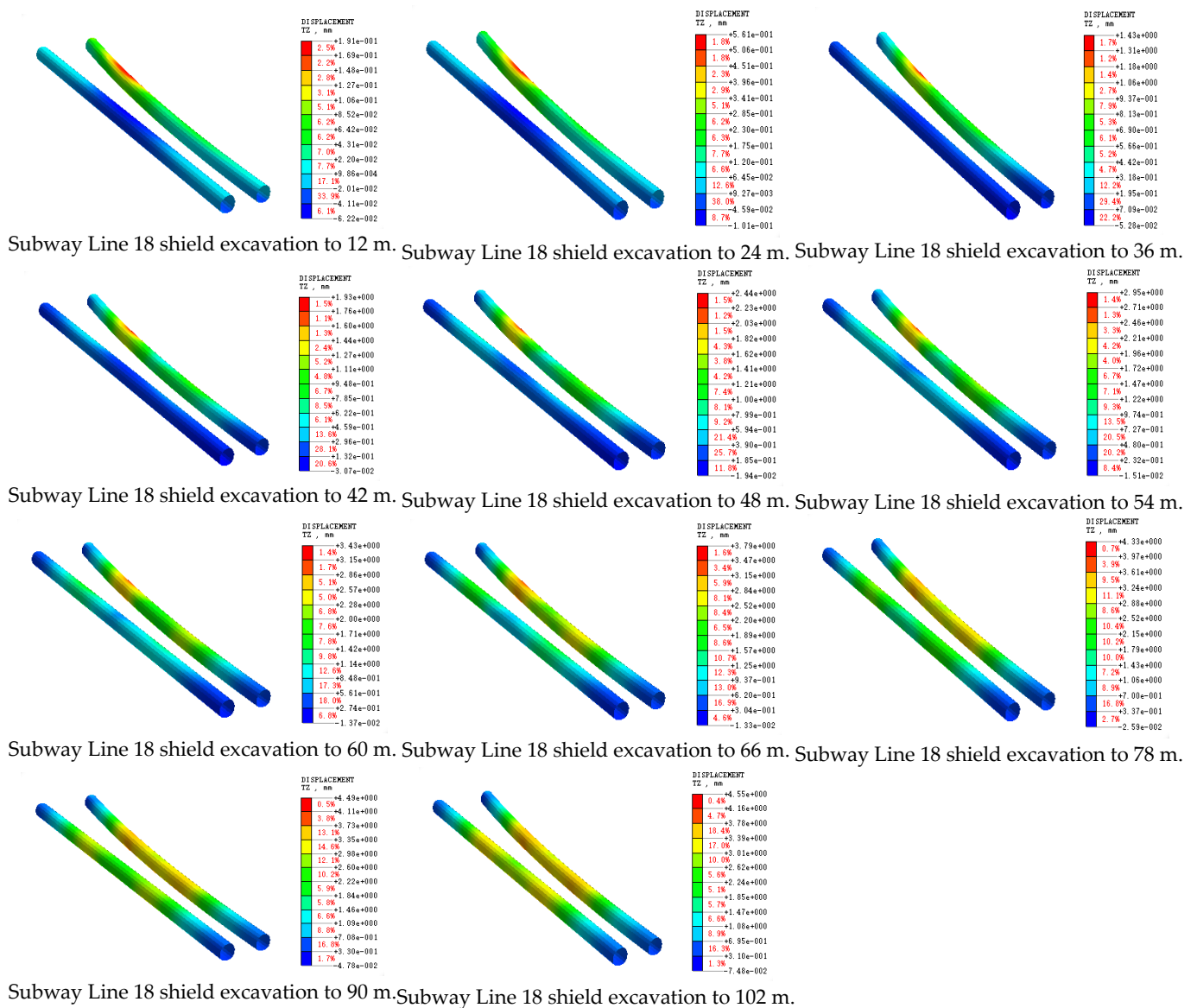


Figure 10. The maximum vertical Z-displacement nephogram of the tunnel structure of Subway Line 5 in the tunneling process of Subway Line 18.

According to the above data, it is easy to identify that in the shield-tunneling process of subway Line 18, the maximum X horizontal displacement, maximum Y horizontal displacement, maximum Z vertical displacement, and maximum total displacement of the tunnel structure of subway Line 5 are 1.09 mm, 3.50 mm, 4.55 mm, and 5.43 mm,

respectively, which are all small amounts. Among them, the maximum Y horizontal displacement is 279.82% of the maximum X horizontal displacement, and the maximum Z vertical displacement is 417.43% of the maximum X horizontal displacement. This means that in the shield-tunneling process of subway Line 18, the displacement along the tunnel direction of subway Line 5 is far less than that in the vertical tunnel direction, and the level of displacement above and below the tunnel is relatively high, which is because the tunnel structure of subway Line 5 is mainly located in the highly weathered argillaceous siltstone layer.

According to Table 2, when the shield construction of the new tunnel is excavated to 102 m, the maximum Y horizontal displacement of the existing tunnel above is 3.5 mm. The settlement of 0.89 mm occurs when the new tunnel is excavated to 24 m; that is, about 40 m away from the existing tunnel, and the settlement is not obvious at this time. When the new tunnel is excavated to 36 m, the settlement value of the existing tunnel is 1.59 mm, the settlement has a certain increasing trend, and the trend is obvious. At this time, the distance from the existing tunnel is 1.4D, which means that the settlement monitoring should be strengthened when the distance between the shield head and the existing tunnel is about 1.5D in the actual construction. When the new tunnel is excavated to 42 m, the excavation position is just below the existing tunnel (the right line of subway Line 5), and the settlement value reaches 2.23 mm, which is about 64% of the maximum settlement during the excavation process simulation. At this time, the settlement trend is more obvious. When the new tunnel is excavated to 66 m, the head of the shield is just below the left line of the existing tunnel, the settlement value is 3.21 mm, and the increase trend gradually slows. When the new tunnel is excavated to 78 m, the settlement value is 3.37 mm, reaching about 96% of the maximum settlement during the excavation process simulation, and the settlement value increases more slowly. It is suggested that necessary local reinforcement treatment be carried out in this area during construction, to ensure the safety of the existing subway.

In order to more intuitively show the maximum X horizontal displacement, maximum Y horizontal displacement, maximum Z vertical displacement, and maximum total displacement of the tunnel structure of subway Line 5 in the shield-tunneling process of subway Line 18, the above data are drawn in the following figure (Figure 11).

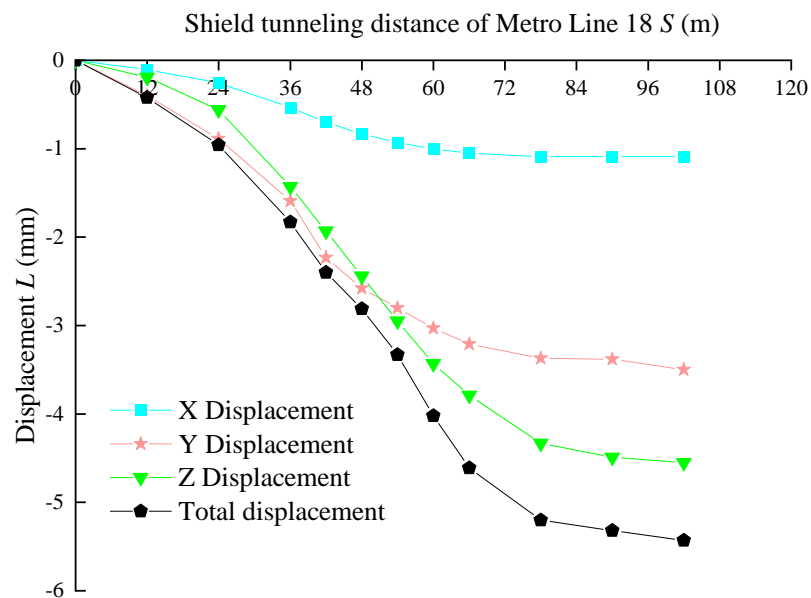


Figure 11. The maximum X horizontal displacement, maximum Y horizontal displacement, maximum Z vertical displacement, and maximum total displacement of the tunnel structure of subway Line 5 caused by the tunneling of subway Line 18.

According to Figure 11, when the shield construction of the new tunnel is promoted, the maximum X horizontal displacement of the existing tunnel above is 1.09 mm. The variation in its settlement value is similar to the maximum Y horizontal displacement, which will not be repeated here. It is worth mentioning that the maximum X horizontal displacement of the existing tunnel above is much smaller than the maximum Y horizontal displacement, and the maximum Z vertical displacement, when the shield construction is promoted. The reason may be that the horizontal X direction is the arched waist position of the existing tunnel, with support and lining.

In order to facilitate the study of the maximum vertical Z-displacement (settlement value) of the existing tunnel above the new tunnel during the promotion of shield construction, Figure 12 is drawn.

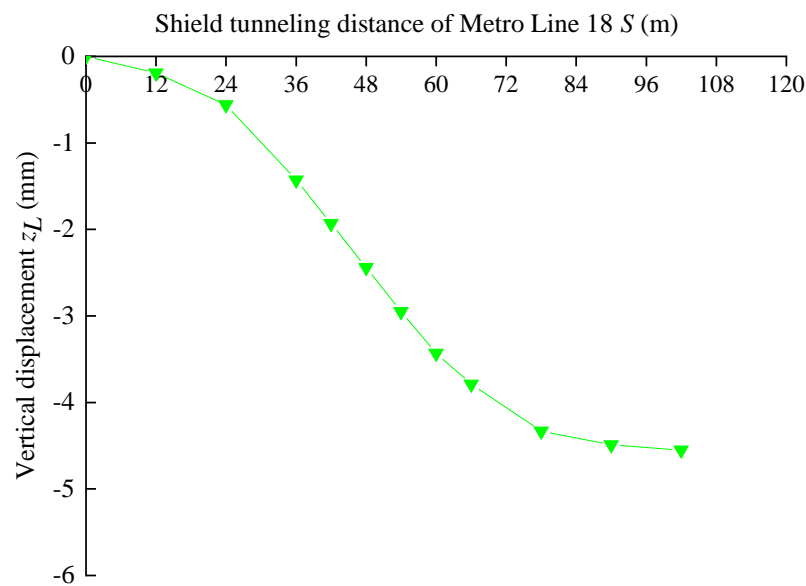


Figure 12. The maximum Z vertical displacement of the existing tunnel above caused by shield tunneling.

As can be seen from Figure 12, when the new tunnel is excavated to 24 m; that is, when it is about 40 m away from the existing tunnel, the settlement of the existing tunnel is 0.56 mm, and the settlement is not obvious at this time. When the new tunnel is excavated to 36 m, the settlement of the existing tunnel is 1.43 mm at this time, the settlement has a certain growth trend, and the trend is obvious. Currently, the distance from the existing tunnel is 1.4D, which means that in the actual construction, the settlement monitoring should be strengthened when the distance between the shield head and the existing tunnel is approximately 1.5D. When the new tunnel is excavated to 42 m, the excavation position is just below the right side of the right line of the existing tunnel, and the settlement reaches 1.93 mm, which is approximately 42% of the maximum settlement during the excavation process simulation. At this time, the settlement trend is more obvious. When the new tunnel is excavated to 66 m, the head of the shield is just below the right side of the left line of the existing tunnel, the settlement is 3.79 mm, and the increase trend gradually slows. When the new tunnel is excavated to 78 m, the head of the shield is just below the left side of the left line of the existing tunnel; the settlement is 4.33 mm, reaching about 95% of the maximum settlement during the excavation process simulation; and the increasing trend in the settlement value slows. This means that settlement monitoring should be strengthened when the tunnel is excavated to 36 m, and that the settlement does not increase significantly until the tunnel is excavated to 78 m. We suggest that a necessary local reinforcement treatment should be carried out in this area during construction, to ensure the safety of the existing subway. Taking the vertical projection of the most dangerous section (the position of the left axis of the existing subway line 5; see subway Line 18 shield excavation to 102 m,

in Figure 10) in the underpass tunnel as the center, beyond the range of 12 m (about 1.5D) before and after the excavation axis of the underpass tunnel, the influence on the structural deformation of the existing tunnel is not obvious, so it can be excavated by normal method.

Based on the above analysis, it is suggested that settlement monitoring should be strengthened within 12 m (about 1.5D) before and after the excavation axis of the underpass tunnel, and it is also necessary to carry out a local reinforcement treatment, to prevent adverse effects on the operation of the existing tunnel. The remainder of the shield excavation area can be constructed according to the normal construction method.

4.2.2. Internal Forces Analysis of Existing Subway Tunnels Caused by New Tunnel Installation

According to the numerical simulation results, the axial force of unit width in the X direction (F_{xx}), and unit width in the Y direction (F_{yy}), for the tunnel structure of subway Line 5 in the shield-tunneling process of subway Line 18, can be obtained. (See Figures 13 and 14). Meanwhile, the internal force data are listed in Table 3.

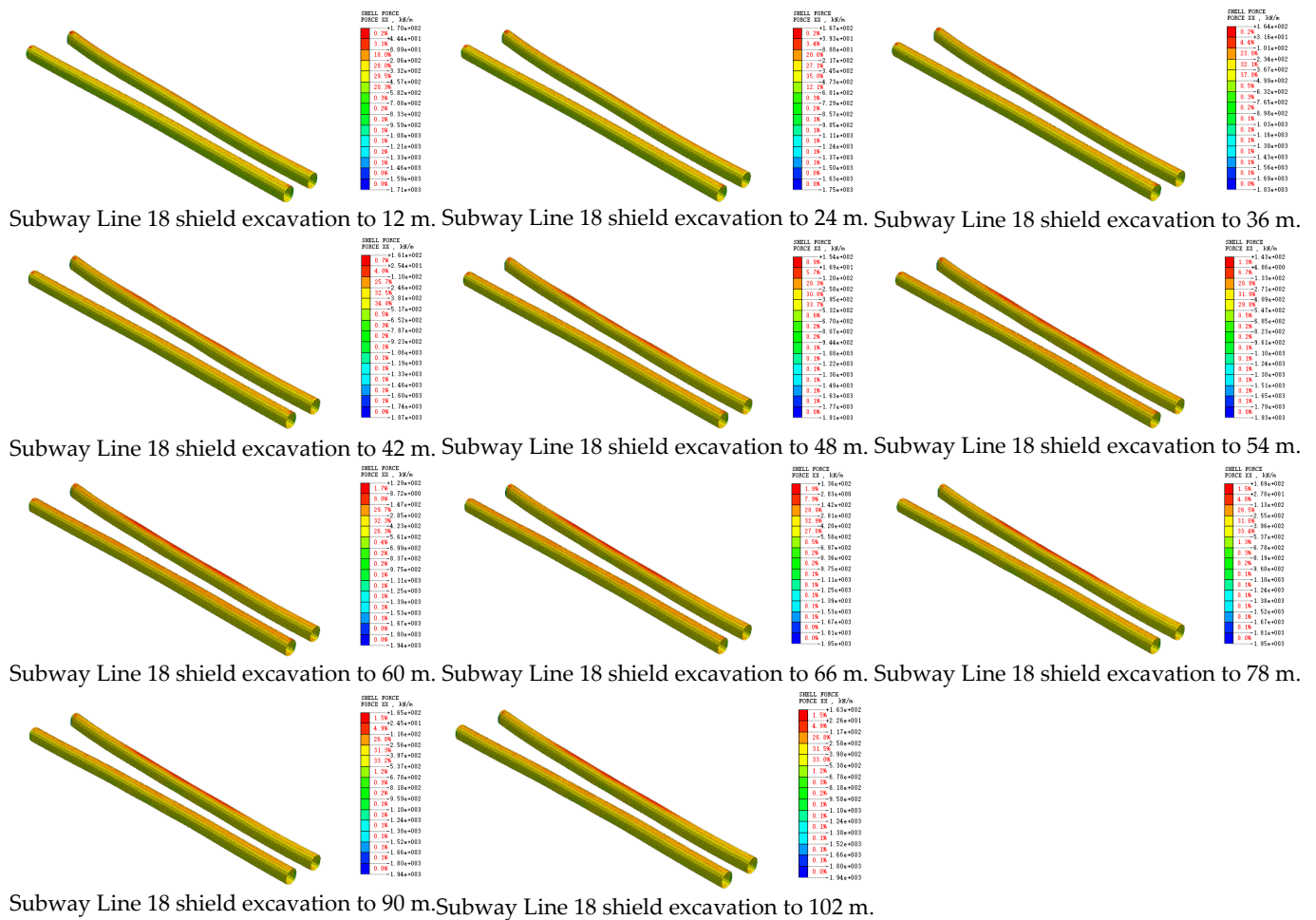


Figure 13. The axial force of unit width in the X direction in the existing tunnel lining caused by the new tunnel’s installation.

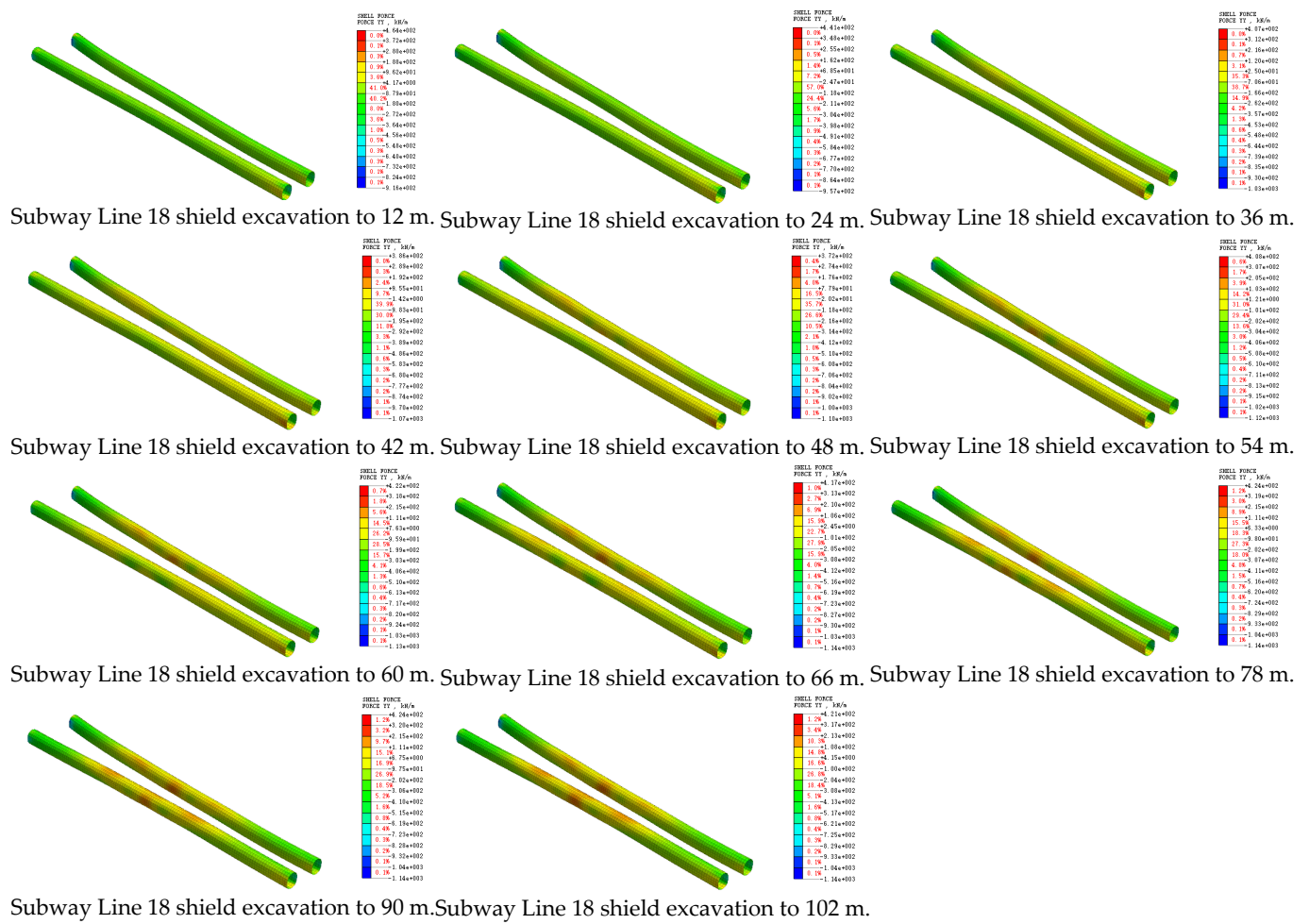


Figure 14. The axial force of unit width in the Y direction in the existing tunnel lining caused by the new tunnel’s installation.

Table 3. Summary of the internal forces of the tunnel structure of subway Line 5 during the shield-tunneling of subway Line 18.

Simulated Working Condition	Internal Forces (kN/m)	
	the Axial Force of Unit Width in the X Direction	the Axial Force of Unit Width in the Y Direction
Construction of subway Line 5 has been completed	1688.77	914.07
Subway Line 18 tunnel excavation 12 m	1720.92	939.71
Subway Line 18 tunnel excavation 24 m	1769.92	981.11
Subway Line 18 tunnel excavation 36 m	1852.52	1052.14
Subway Line 18 tunnel excavation 42 m	1902.04	1094.79
Subway Line 18 tunnel excavation 48 m	1939.99	1126.64
Subway Line 18 tunnel excavation 54 m	1965.26	1147.56
Subway Line 18 tunnel excavation 60 m	1980.09	1160.14
Subway Line 18 tunnel excavation 66 m	1987.24	1166.98
Subway Line 18 tunnel excavation 78 m	1988.23	1171.35
Subway Line 18 tunnel excavation 90 m	1981.16	1170.17
Subway Line 18 tunnel excavation 102 m	1976.62	1171.49

According to Figure 13 and Table 3, the maximum axial force of the element width in the X direction is concentrated above the existing tunnel, while the existing tunnel has a lower side-wall concentration, and receives less axial force. With the advance of the shield

of subway Line 18, the maximum axial force of the unit width in the X direction gradually increases, until the shield of subway Line 18 is excavated to 78 m, reaching the maximum value (1988.23 kN/m) in the entire excavation process. As the shield excavation of subway Line 18 continues, the maximum axial force of the unit width in the X direction gradually decreases, but the reduction is small (less than 0.4%). It is worth noting that when the shield propulsion of subway line 18 is between 24 m and 36 m, the maximum axial force of the unit width in the X direction increases the most (82.6 kN/m), which indicates that the shield of subway Line 18 has approached the tunnel of subway Line 5 at this time.

According to Figure 14 and Table 3, the maximum axial force of the element width in the Y direction is concentrated in the middle part of the existing tunnel, while the two ends of the existing tunnel are less concentrated, and suffer less axial force. With the advance of the shield of subway Line 18, the maximum axial force of the element width in the Y direction gradually increases, until the shield of subway Line 18 is excavated to 78 m, reaching the maximum value of 1171.35 kN/m in the whole excavation process. As the shield excavation of subway Line 18 continues, the maximum axial force of the element width in the Y direction begins to fluctuate, but the fluctuation amplitude is very small (less than 0.2%). It is worth noting that when the shield propulsion of subway line 18 is between 24 m and 36 m, the maximum axial force of the unit width in the X direction increases the most (71.03 kN/m), which indicates that the shield of subway Line 18 has approached the tunnel of subway Line 5 at this time.

4.2.3. Comparison between Calculated Values and Theoretical Values of Loose Soil Pressure

According to the above working conditions, the maximum Z vertical displacement calculated is 4.55 mm during the excavation process simulation. Because the numerical calculation does not take into account the existing overlying subway operation activities, and the periodic load of vehicles on the road surface, this value should be smaller than the measured value, and the influence range narrower than the measured value. According to the theory of loosening earth pressure (Terzaghi [31]), the roof loose half-width was calculated as:

$$B_1 = R_0 \cot\left(\frac{\pi/4 + \varphi/2}{2}\right), \quad (13)$$

where R_0 is outer radius of the segment, 6.1 m; and φ is the internal friction angle of the rock mass, set at 30° , according to Table 1.

According to Equation (13), B_1 is 10.56 m, about $1.25D$, which is smaller than the simulated value. This is because the arch effect is considered in the theory of loose soil pressure, so the calculated influence width is relatively smaller. Based on the above analysis, the model in this paper is reasonable.

4.2.4. Comparison of Field Monitoring Results with Numerical Simulation

According to the actual monitoring data, the maximum settlement value of horizontal displacement in the right line hole is 2.44 mm, and the maximum settlement value of vertical displacement in the right line hole is 4.86 mm. The maximum settlement value of horizontal displacement in the left line hole is 3.71 mm, and the maximum settlement value of vertical displacement in the left line hole is 3.82 mm. The maximum horizontal displacement in the hole, and the maximum vertical displacement in the hole, correspond to the maximum displacement in the X direction, and the maximum displacement in the z direction, respectively, in the numerical simulation. It can be seen in Table 2 that the maximum displacement in the X direction, and the maximum displacement in the z direction, in the numerical simulation, are 1.09 and 4.55 mm, respectively, which is very close to the actual monitoring data. In fact, we are mainly concerned about the maximum settlement value of vertical displacement in the tunnel, and it is easy to find that the difference between the measured value and the numerical simulation result is only 6.38%. It shows that the numerical model is more reliable. However, there are many assumptions in the modeling of this model, so there must be some differences from the actual monitoring

data. These assumptions generally cause the numerical simulation result to be smaller than the measured value.

4.2.5. Conclusion of Three-Dimensional Numerical Simulation and Field Monitoring Results

Based on the theory of loosening earth pressure, the half-width of the roof looseness is calculated to be 10.56 m (about $1.25D$), which is smaller than the numerical simulation value, which agrees with the hypothesis of the theory. The numerical model in this paper is considered to be reliable.

In the shield-tunneling process of subway Line 18, the maximum X horizontal displacement value, maximum Y horizontal displacement value, maximum Z vertical displacement value, and maximum total displacement value of the subway Line 5 section tunnel structure are 1.09 mm, 3.50 mm, 4.55 mm, and 5.43 mm. Among them, the maximum Y horizontal displacement is 279.82% of the maximum X horizontal displacement, and the maximum Z vertical displacement is 417.43% of the maximum X horizontal displacement. In the shield-tunneling process of subway Line 18, the displacement along the tunnel direction of subway Line 5 is far smaller than that in the vertical tunnel direction, and the displacement above and below the tunnel is relatively large. This is because the tunnel structure of subway Line 5 is mainly in the strongly weathered argillaceous siltstone layer.

In addition, with the vertical projection of the most dangerous section in the underpass tunnel as the center, the influence on the structural deformation of the existing tunnel is not obvious beyond the range of 12 m (about $1.5D$) before and after the excavation axis of the underpass tunnel, and the tunnel can be excavated using the normal method. The settlement monitoring should be strengthened when the new tunnel is excavated to 36 m, and the settlement does not increase significantly until the tunnel is excavated to 78 m. It is suggested that a necessary local reinforcement treatment is carried out for the shield construction area during construction, to ensure the safety of the existing subway.

The maximum displacement in the X direction, and the maximum displacement in the z direction in the numerical simulation are very close to the actual monitoring data. However, there are many assumptions in the modeling of this model, which generally cause the numerical simulation results to be smaller than the measured values.

5. Safety Measures and Suggestions

By referring to the engineering geological data of the subway Line 18 and Line 5 tunnels, combined with the shield-tunneling characteristics of subway Line 18, and the tunnel-structure characteristics of the existing subway Line 5, we can see that the tunneling of subway Line 18 under the tunnel structure of subway line 5 will result in the unloading of the underside of the tunnel structure of subway Line 5, thus changing its stress and deformation state. This will affect the normal operation of subway Line 5.

In order to ensure the safety of the tunnel structure and operation in the section of the existing subway Line 5, the following suggestions are proposed. (1) In the construction process of the project, the structural displacement monitoring data should be closely combined with the monitoring data related to shield construction, and the inversion calculation of the stratum calculation parameters should be carried out, when necessary. (2) According to the safety protection experience and relevant norms of similar subway structures in China, and combined with the preliminary analysis results of the status quo of subway structures, the control value for subway structure displacement is preliminarily proposed as 6.00 mm. (3) It is suggested that settlement monitoring should be strengthened within 12 m (about $1.5D$) before and after the excavation axis of the underpass tunnel. It is also necessary to carry out a local grouting reinforcement treatment, to prevent adverse effects on the operation of the existing tunnel. (4) Earth pressure control is required; the pressure in the soil bin must be balanced with the water pressure on the excavation face to maintain the stability of the soil mass on the excavation face, so as to reduce the overhead influence on the subway Line 5 tunnel. (5) The propulsion speed must be controlled; the shield machine should be advanced at a constant and slow speed, and the shield-tunneling

speed should be controlled at 20~30 mm/min in the process of under-crossing the subway Line 5 tunnel. (6) During the construction of the project, the displacement monitoring of the tunnel structure adjacent to the affected area should be strengthened, for the timely monitoring of the safety status of the tunnel structure. If necessary, the design parameters of the foundation structure should be strengthened according to the monitoring information, and the shield-tunneling construction scheme should be adjusted.

6. Conclusions

In this paper, the influence of tunnel construction on the deformation of the overlying strata is analyzed, and the formula for estimating the horizontal and longitudinal settlement of strata at depth z below the surface caused by the excavation of a double-line parallel tunnel is deduced. Based on the engineering geological data of the subway Line 18 and Line 5 tunnels, combined with the shield-tunneling of subway Line 18 and the tunnel-structure characteristics of subway Line 5, the existing tunnel structure is calculated and analyzed according to a series of three-dimensional numerical simulations, and some suggestions are put forward for the safe construction of subway Line 18. The specific conclusions are as follows:

(1) Based on the superposition principle, the formulae for estimating the surface longitudinal settlement caused by the excavation of a double-line parallel tunnel, and the formulae for estimating the horizontal and longitudinal settlement of strata at depth z below the surface, are obtained.

(2) The tunnel structure of subway Line 5 and Line 18 is mainly located in the highly weathered argillaceous siltstone stratum, and slightly weathered argillaceous siltstone stratum, respectively. The tunnel of Line 18 is located in the relatively safe strata, and it is considered that the construction conditions are good, and the construction is safe.

(3) According to numerical simulation analysis, in the shield-tunneling process of subway line 18, the maximum X horizontal displacement, maximum Y horizontal displacement, and maximum Z vertical displacement of the tunnel structure of subway Line 5 are 1.09, 3.50, and 4.55 mm, respectively. It is considered that the influence of the shield tunneling of subway Line 18 on the tunnel structure of subway Line 5 is relatively controllable. It does not affect its structural and operational safety.

(4) The calculated maximum vertical displacement is 4.55 mm during the excavation process simulation. It is suggested that settlement monitoring should be strengthened within 12 m (about $1.5D$) before and after the excavation axis of the underpass tunnel. It is also necessary to carry out a local reinforcement treatment, to prevent adverse effects on the operation of the existing tunnel.

Author Contributions: Conceptualization, L.Z. and D.Z.; methodology, C.L., J.Z. and H.Y.; writing—original draft preparation, L.Z.; writing—review and editing, L.Z. and D.Z. All authors have read and agreed to the published version of the manuscript.

Funding: This research was funded by the National Natural Science Foundation of China, grant numbers 52074116 and 51804113. The financial support is greatly appreciated.

Data Availability Statement: The data presented in this study are available on request from the corresponding author. The data are not publicly available due to their complexity.

Conflicts of Interest: The authors declare no conflict of interest.

References

1. Ma, Z.; Zuo, J.; Zhu, F.; Liu, H.; Xu, C. Non-orthogonal Failure Behavior of Roadway Surrounding Rock Subjected to Deep Complicated Stress. *Rock Mech. Rock Eng.* **2023**. [[CrossRef](#)]
2. Choi, J.; Lee, S. Influence of existing tunnel on mechanical behavior of new tunnel. *KSCE J. Civ. Eng.* **2010**, *14*, 773–783. [[CrossRef](#)]
3. Zhang, Z.; Huang, M. Geotechnical influence on existing subway tunnels induced by multiline tunneling in Shanghai soft soil. *Comput. Geotech.* **2014**, *56*, 121–132. [[CrossRef](#)]
4. Huang, L.; Ma, J.; Lei, M.; Liu, L.; Lin, Y.; Zhang, Z. Soil-water inrush induced shield tunnel lining damage and its stabilization: A case study. *Tunn. Undergr. Space Technol.* **2020**, *97*, 103290. [[CrossRef](#)]

5. Lin, Y.; Ma, J.; Lai, Z.; Huang, L.; Lei, M. A FDEM approach to study mechanical and fracturing responses of geo-materials with high inclusion contents using a novel reconstruction strategy. *Eng. Fract. Mech.* **2023**, *282*, 109171. [[CrossRef](#)]
6. Lin, Y.; Wang, X.; Ma, J.; Huang, L. A finite-discrete element based approach for modelling the hydraulic fracturing of rocks with irregular inclusions. *Eng. Fract. Mech.* **2022**, *261*, 108209. [[CrossRef](#)]
7. Xu, Q.; Zhu, H.; Ma, X.; Ma, Z.; Li, X.; Tang, Z.; Zhuo, K. A case history of shield tunnel crossing through group pile foundation of a road bridge with pile underpinning technologies in Shanghai. *Tunn. Undergr. Space Technol.* **2015**, *45*, 20–33. [[CrossRef](#)]
8. Esen Sze, Y.; Jim Yee, T.; Henry Kim, I.; Osborne, N.; Chang, K.; Siew, R. Tunnelling undercrossing existing live MRT tunnels. *Tunn. Undergr. Space Technol.* **2016**, *57*, 241–256. [[CrossRef](#)]
9. Lin, Y.; Yin, Z.; Wang, X.; Huang, L. A systematic 3D simulation method for geomaterials with block inclusions from image recognition to fracturing modelling. *Theor. Appl. Fract. Mech.* **2022**, *117*, 103194. [[CrossRef](#)]
10. Liu, H.; Small, J.; Carter, J.; Williams, D. Effects of tunnelling on existing support systems of perpendicularly crossing tunnels. *Comput. Geotech.* **2009**, *36*, 880–894. [[CrossRef](#)]
11. Ng, C.; Fong, K.; Liu, H. The effects of existing horseshoe-shaped tunnel sizes on circular crossing tunnel interactions: Three-dimensional numerical analyses. *Tunn. Undergr. Space Technol.* **2018**, *77*, 68–79. [[CrossRef](#)]
12. Yang, F.; Liu, J.; Liu, Y.; Zhang, L. Research on Spacing Effect of The Construction of Shield Tunnels undercrossed Existing Tunnels at Close Distance. *IOP Conf. Ser. Earth Environ. Sci.* **2018**, *189*, 022086. [[CrossRef](#)]
13. Cao, R.; Peng, L.; Zhao, Y. Control of Strata Deformation in Subway Interval Tunnels Crossing a High-Speed Rail Shield Tunnel at a Short Distance. *Arab. J. Sci. Eng.* **2021**, *46*, 5013–5022. [[CrossRef](#)]
14. Chen, F.; Wang, L.; Zhang, W. Reliability assessment on stability of tunnelling perpendicularly beneath an existing tunnel considering spatial variabilities of rock mass properties. *Tunn. Undergr. Space Technol.* **2019**, *88*, 276–289. [[CrossRef](#)]
15. Huang, Z.; Zhang, C.; Fu, H.; Deng, H.; Ma, S.; Fu, J. Numerical Study on the Disturbance Effect of Short-Distance Parallel Shield Tunnelling Undercrossing Existing Tunnels. *Adv. Civ. Eng.* **2020**, *2020*, 8810658. [[CrossRef](#)]
16. Liang, J.; Tang, X.; Wang, T.; Lin, W.; Yan, J.; Fu, C. Analysis for Ground Deformation Induced by Undercrossed Shield Tunnels at a Small Proximity Based on Equivalent Layer Method. *Sustainability* **2022**, *14*, 9972. [[CrossRef](#)]
17. Lu, Y.; Huang, W. Numerical Simulation of Dynamic Response Law of Intersecting Metro Tunnels in Upper and Lower Strata. *Geotech. Geol. Eng.* **2020**, *38*, 3773–3785. [[CrossRef](#)]
18. Fang, Q.; Du, J.; Li, J.; Zhang, D.; Cao, L. Settlement characteristics of large-diameter shield excavation below existing subway in close vicinity. *J. Cent. South Univ.* **2021**, *28*, 882–897. [[CrossRef](#)]
19. Islam, M.; Iskander, M. Twin tunnelling induced ground settlements: A review. *Tunn. Undergr. Space Technol.* **2021**, *110*, 103614. [[CrossRef](#)]
20. Hasan, M.; Husaini; Abdullah, N. Deformation and crack analysis of tunnel structure subjected to static distributed load using Pseudoshell model. *IOP Conf. Ser. Mater. Sci. Eng.* **2019**, *523*, 012034. [[CrossRef](#)]
21. Luo, C.; Cheng, Y.; Bai, Z.; Shen, T.; Wu, X.; Wang, Q. Study on Deformation Law of Subway Construction under Passing Existing Line in Short Distance. *Adv. Civ. Eng.* **2021**, *2021*, 6626927. [[CrossRef](#)]
22. Weng, X.; Yu, H.; Niu, H.; Hu, J.; Han, W.; Huang, X. Interactive effects of crossing tunnel construction on existing tunnel: Three-dimensional centrifugal test and numerical analyses. *Transp. Geotech.* **2022**, *35*, 100789. [[CrossRef](#)]
23. Lai, H.; Zhao, X.; Kang, Z.; Chen, R. A new method for predicting ground settlement caused by twin-tunneling under-crossing an existing tunnel. *Environ. Earth Sci.* **2017**, *76*, 726. [[CrossRef](#)]
24. Yin, M.; Jiang, H.; Jiang, Y.; Sun, Z.; Wu, Q. Effect of the excavation clearance of an under-crossing shield tunnel on existing shield tunnels. *Tunn. Undergr. Space Technol.* **2018**, *78*, 245–258. [[CrossRef](#)]
25. Lin, X.; Chen, R.; Wu, H.; Cheng, H. Deformation behaviors of existing tunnels caused by shield tunneling undercrossing with oblique angle. *Tunn. Undergr. Space Technol.* **2019**, *89*, 78–90. [[CrossRef](#)]
26. Gan, X.; Yu, J.; Gong, X.; Liu, N.; Zheng, D. Behaviours of existing shield tunnels due to tunnelling underneath considering asymmetric ground settlements. *Undergr. Space* **2022**, *7*, 882–897. [[CrossRef](#)]
27. Peck, R. Deep excavations and tunnelling in soft ground. In Proceedings of the 7th International Conference on Soil Mechanics and Foundation Engineering, Mexico City, Mexico, 25–31 August 1969; pp. 225–290.
28. Attewell, P.; Woodman, J. Predicting the dynamics of ground settlement and its derivatives caused by tunneling in soil. *Ground Eng.* **1982**, *15*, 13–22, 36.
29. New, B.; O'Reilly, M. Tunnelling induced ground movements: Predicting their magnitude and effects (invited review paper). In Proceedings of the 4th International Conference on Ground Movements and Structures, Cardiff, UK, 8–11 July 1991; Pentech Press: London, UK, 1991; pp. 671–690.
30. Liu, J.; Hou, X. *Shield Tunnel*; China Railway Publishing House: Beijing, China, 1991.
31. Terzaghi, K. *Theoretical Soil Mechanics*; John Wiley & Sons: New York, NY, USA, 1943.

Disclaimer/Publisher's Note: The statements, opinions and data contained in all publications are solely those of the individual author(s) and contributor(s) and not of MDPI and/or the editor(s). MDPI and/or the editor(s) disclaim responsibility for any injury to people or property resulting from any ideas, methods, instructions or products referred to in the content.